Precision Tracking for an H-Frame XY Positioning System

Richard J. Vaccaro[1], Yacine Boudria[1], Musa Jouaneh[2], and Ahmed S. Zaki[3]

***Abstract*— The problem considered is the design of a digital control system for precision tracking control of an H-frame, belt-driven, XY positioning system, which is a fully coupled MIMO plant. The first step is to design a feedback control system using standard linear quadratic regulator techniques with integral control. The second step is to design a feedforward command shaping filter (CSF). The derivation of the CSF, based on a novel approximation, is provided. Experimental results are given for precision tracking with a prototype H-frame positioning system. It is shown that the CSF extends the precision-tracking bandwidth from 2 Hz for the feedback loop alone, to 10 Hz for the combination of the CSF and feedback loop.**

I. INTRODUCTION

Feedback control systems with integral control have the desirable property of zero steady-state error to constant reference inputs. However, the precision-tracking bandwidth of a feedback control system may be small. By precision tracking, we mean the ability of a control system to keep the error between the reference signals and the plant outputs less than a small error bound over the entire duration of the reference signals. A typical feedback control system designed for zero steady-state error will provide precision tracking only for low-frequency reference signals. That is, precision tracking is achieved only for reference signals whose frequency content is within some band of low frequencies. The precision-tracking bandwidth can be increased by using larger feedback gains. However, such high-gain feedback is problematic in hardware systems such as the H-frame system considered in this paper due to sensor noise and unmodeled high-frequency dynamics. Instead of increasing the feedback gains, the approach taken in this paper is to design a feedforward filter that increases the precision-tracking bandwidth of the system.

The outline of the paper is as follows. Section II reviews the development of a standard state-feedback tracking system with integral control, which is used as a baseline controller. Section III deals with the design of a MIMO system command shaping filter (CSF) that is used in cascade with the feedback loop to extend the precision-tracking bandwidth. The relationship to previous work is also discussed. Section IV provides experimental results using the proposed method with an H-frame XY positioning system. It is shown that the CSF extends the precision-tracking bandwidth from 2 Hz, for the feedback loop alone, to 10 Hz for the combination of the CSF and feedback loop. Conclusions are given in Section V.

[1]Department of Electrical, Computer, & Biomedical Engineering, [2]Department of Mechanical, Industrial, & Systems Engineering, University of Rhode Island, Kingston, RI 02881, USA, [3]Naval Undersea Warfare Center, Division Newport, Newport, RI 02840. vaccaro@ele.uri.edu, yaciboud@gmail.com, jouaneh@egr.uri.edu , ahmed.zaki@navy.mil

II. FEEDBACK TRACKING SYSTEM

Consider an nth-order linear, p-input, p-output plant with state-space model

$$\begin{aligned} \dot{\mathbf{x}} &= \mathbf{A}\mathbf{x} + \mathbf{B}\mathbf{u} \\ \mathbf{y} &= \mathbf{C}\mathbf{x}. \end{aligned} \tag{1}$$

For digital control with sampling interval T seconds the zero-order hold (ZOH) equivalent plant model is

$$\begin{aligned} \mathbf{x}[k+1] &= \mathbf{\Phi}\mathbf{x}[k] + \mathbf{\Gamma}\mathbf{u}[k] \\ \mathbf{y}[k] &= \mathbf{C}\mathbf{x}[k] \end{aligned} \tag{2}$$

where

$$\mathbf{\Phi} = e^{\mathbf{A}T} \text{ and } \mathbf{\Gamma} = \int_0^T e^{\mathbf{A}\tau}\mathbf{B}\, d\tau. \tag{3}$$

In order to design a control system in which $\mathbf{y}[k]$ tracks a class of reference signals $\{\mathbf{w}[k]\}$ with zero steady-state error, we must use additional dynamics (see Fig. 1):

$$\mathbf{x}_a[k+1] = \mathbf{\Phi}_a\mathbf{x}_a[k] + \mathbf{\Gamma}_a\mathbf{e}[k] \tag{4}$$

where the eigenvalues of $\mathbf{\Phi}_a$ are the poles of the z-transform of $\mathbf{w}[k]$ [2,3]. For tracking step signals an eigenvalue at $z = 1$ is required, which gives digital integral control. For a MIMO tracking system, the additional dynamics pole(s) must be replicated up to the number of plant outputs. For example, to track step signals for a plant with p outputs the additional dynamics are given by a parallel combination of p digital integrators:

$$\mathbf{\Phi}_a = \mathbf{I}_p, \quad \mathbf{\Gamma}_a = \mathbf{I}_p. \tag{5}$$

A digital state-feedback tracking system is shown in Fig. 1.

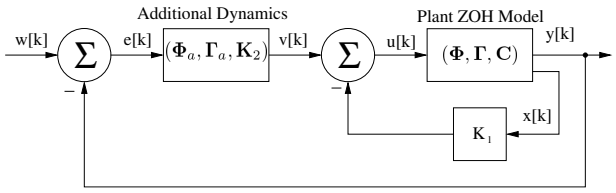

Fig. 1. A digital state-space tracking system.

In order to compute the state-feedback gain matrix $\mathbf{K}_1$ and the integrator gain matrix $\mathbf{K}_2$, a design model consisting of the cascade of the plant followed by the additional dynamics is needed [3]. This design model is given by:

$$\mathbf{\Phi}_d = \begin{bmatrix} \mathbf{\Phi} & \mathbf{0} \\ \mathbf{\Gamma}_a\mathbf{c} & \mathbf{\Phi}_a \end{bmatrix}, \ \mathbf{\Gamma}_d = \begin{bmatrix} \mathbf{\Gamma} \\ \mathbf{0} \end{bmatrix}. \tag{6}$$

A feedback gain matrix $\mathbf{K}_d$ may be obtained, for example, using the discrete-time linear quadratic regulator formulas. The matrices $\mathbf{K}_1$ and $\mathbf{K}_2$ are obtained by partitioning $\mathbf{K}_d$,

$$\mathbf{K}_d = [\,\mathbf{K}_1 \quad \mathbf{K}_2\,], \tag{7}$$

where $\mathbf{K}_1$ consists of the first n columns of $\mathbf{K}_d$. The precision-tracking bandwidth of the system shown in Fig. 1 can be increased by cascading it with a feedforward filter. The derivation of this filter is given next.

III. Command Shaping Filter Design

The closed-loop system from $\mathbf{w}[k]$ to $\mathbf{y}[k]$ in Fig. 1 will be denoted by following state-space model:

$$\begin{aligned} \mathbf{x}_c[k+1] &= \mathbf{\Phi}_c\mathbf{x}_c[k] + \mathbf{\Gamma}_c\mathbf{w}[k] \\ \mathbf{y}[k] &= \mathbf{C}_c\mathbf{x}[k] \end{aligned} \tag{8}$$

where

$$\mathbf{x}_c[k] = \begin{bmatrix} \mathbf{x}[k] \\ \mathbf{x}_a[k] \end{bmatrix}. \tag{9}$$

The design of the command shaping filter begins by attempting to invert the model for the closed-loop system. Consider advances of the plant output, $\mathbf{y}[k+r]$. Let r be the smallest integer for which $\mathbf{C}\mathbf{\Phi}_c^{r-1}\mathbf{\Gamma}$ is a nonzero matrix. Then it can be shown that

$$\mathbf{y}[k+r] = \mathbf{C}\mathbf{\Phi}_c^{r}\mathbf{x}[k] + \mathbf{C}\mathbf{\Phi}_c^{r-1}\mathbf{\Gamma}\mathbf{w}[k]. \tag{10}$$

We assume that the matrix-product multiplying $\mathbf{w}[k]$ is invertible. Define

$$\mathbf{D}_f = (\mathbf{C}\mathbf{\Phi}_c^{r-1}\mathbf{\Gamma})^{-1}. \tag{11}$$

The (10) may be rearranged to obtain

$$\mathbf{v}[k] = -\mathbf{D}_f\mathbf{C}\mathbf{\Phi}_c^{r}\mathbf{x}[k] + \mathbf{D}_f\mathbf{y}[k+r]. \tag{12}$$

This equation may be substituted into the first equation of (8) to obtain

$$\begin{aligned} \mathbf{x}[k+1] &= \mathbf{\Phi}_f\mathbf{x}[k] + \mathbf{\Gamma}_f\mathbf{y}[k+r] \\ \mathbf{w}[k] &= \mathbf{C}_f\mathbf{x}_c[k] + \mathbf{D}_f\mathbf{y}[k+r] \end{aligned} \tag{13}$$

where $\mathbf{D}_f$ is given by (11) and

$$\begin{aligned} \mathbf{C}_f &= -\mathbf{D}_f\mathbf{C}\mathbf{\Phi}_c^{r} \\ \mathbf{\Phi}_f &= \mathbf{\Phi}_c + \mathbf{\Gamma}\mathbf{C}_f \\ \mathbf{\Gamma}_f &= \mathbf{D}_f\mathbf{\Gamma}. \end{aligned} \tag{14}$$

Equation (13) shows that the system $(\mathbf{\Phi}_f, \mathbf{\Gamma}_f, \mathbf{C}_f, \mathbf{D}_f)$, which will be called the *command shaping filter* (CSF), produces the signal $\mathbf{w}[k]$ from the advanced plant output $\mathbf{y}[k+r]$, which inverts the closed-loop system model in (8) with a delay of r samples. That is, the cascade of the CSF (13) and the closed-loop system (8) is a pure delay of r samples on each output signal. Thus, the CSF may be used as a feedforward filter in the system in Fig. 1 to obtain theoretically perfect tracking with a delay of r samples.

The preceding development is useful only if the CSF is stable. The poles of the CSF will include the transmission zeros of the modified plant. If the plant itself is nonminimum phase, some of the poles of the CSF will be outside the unit circle. Even if the continuous-time plant is minimum phase, some of the eigenvalues of the CSF may be outside the unit circle due to the presence of "sampling zeros." Whatever the cause of unstable eigenvalues of the CSF, additional calculations are needed to obtain a stable approximate inverse for the closed-loop system, as shown next.

A. Adding Additional Advances

Consider adding s more advances to the r advances shown in (10). The result is, with $d = r + s$,

$$\mathbf{y}[k+d] = \mathbf{C}\mathbf{\Phi}_c^{d}\mathbf{x}[k] + \sum_{i=0}^{s}\mathbf{C}\mathbf{\Phi}_c^{d-i-1}\mathbf{w}[k+i]. \tag{15}$$

We can then make the approximation that

$$\mathbf{w}[k+i] \approx \mathbf{w}[k],\ i = 1, \cdots, s. \tag{16}$$

Substituting this into (15) yields

$$\mathbf{y}[k+d] \approx \mathbf{C}\mathbf{\Phi}_c^{d}\mathbf{x}_c[k] + \mathbf{D}_f^{-1}\mathbf{w}[k] \tag{17}$$

where

$$\mathbf{D}_f = \left(\sum_{i=0}^{s}\mathbf{C}\mathbf{\Phi}_c^{d-i-1}\mathbf{\Gamma}\right)^{-1}. \tag{18}$$

Using the same procedure as before (i.e. solving (17) for $\mathbf{w}[k]$ and substituting into (8)) we obtain athe CSF$(\mathbf{\Phi}_f, \mathbf{\Gamma}_f, \mathbf{C}_f, \mathbf{D}_f)$ with $\mathbf{D}_f$ given by (18) and

$$\begin{aligned} \mathbf{C}_f &= -\mathbf{D}_f\mathbf{C}\mathbf{\Phi}_c^{d} \\ \mathbf{\Phi}_f &= \mathbf{\Phi}_c + \mathbf{\Gamma}\mathbf{C}_f \\ \mathbf{\Gamma}_f &= \mathbf{D}_f\mathbf{\Gamma}. \end{aligned} \tag{19}$$

Note that, for sufficiently large d, this CSF will be stable. The CSF state-transition matrix is $\mathbf{\Phi}_f = \mathbf{\Phi}_c + \mathbf{\Gamma}_c\mathbf{C}_f$ and the entries of $\mathbf{C}_f = -\mathbf{D}_f\mathbf{C}_c\mathbf{\Phi}_c^{d}$ can be made arbitrarily small by increasing d. Thus, the eigenvalues of $\mathbf{\Phi}_f$ will move towards the eigenvalues of $\mathbf{\Phi}_c$ and become stable for sufficiently large d. The value of d is chosen to be the smallest integer for which the resulting $\mathbf{\Phi}_f$ has all its eigenvalues inside the unit circle. That is,

$$d^* = \text{smallest } d \text{ s. t. } \max(\text{abs}(\text{eig}(\mathbf{\Phi}_c - \mathbf{\Gamma}\mathbf{D}_f\mathbf{C}\mathbf{\Phi}_c^{d}))) < R, \tag{20}$$

where R is a user-defined maximum pole radius, e.g. $R = 0.99$.

The cascade of this CSF with the modified plant will not be a pure delay due to the approximation in (16). That approximation is exact at dc and the approximation error increases with increasing frequency of the signal $\mathbf{w}[k]$. The frequency range over which the CSF provides an accurate inversion must be evaluated by looking at the Bode plot of the cascade of the CSF and closed-loop system. A precision tracking system is obtained by inserting a feedforward CSF into Fig. 1 and accounting for the delay of d samples. The result is shown in Fig. 2.

When using a feedforward CSF one must be concerned with the effects of plant model uncertainty. Although these effects are not analyzed in this paper, we note that the feedback loop in Fig. 2 reduces these effects. In other words, the uncertainty of the closed-loop system from $\mathbf{w}[k]$ to $\mathbf{y}[k]$

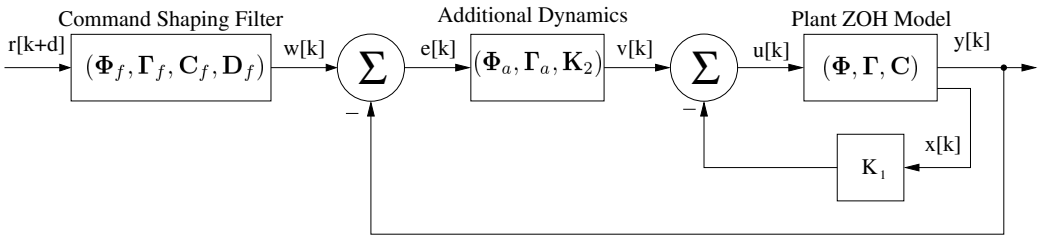

Fig. 2. Digital tracking system model with command shaping filter.

is smaller than the uncertainty in the plant model due to the effects of feedback and integral control. The design of the state-feedback loop is done, in part, to reduce the effects of plant model uncertainty.

B. Relationship to Previous Work

The command shaping filter derived in the previous subsection is an approximate inverse for a non-minimum phase closed-loop system using a d-sample advance of the reference input. The approximation, based on (16), is very good over a range of frequencies that can be evaluated from a Bode plot of the cascade of the CSF and closed-loop system.

The problem of inversion of a non-minimum phase system has been considered previously in the literature [4]. For example, [5] completely solves the theoretical problem of inverting non-minimum phase discrete-time MIMO systems. It is shown that perfect inversion for such systems requires an infinite number of "preaction" samples (the number d in our notation). Truncation to a finite preaction time can be done in such a way as to preserve almost perfect tracking over the entire Nyquist band of frequencies. However, the number of preaction samples needed by this approach must be "significantly greater than the maximum time constant associated to the inverses of the controlled system invariant zeros." Thus, large preaction times will be needed for systems containing one or more zeros near the unit circle. The H-frame system that is the focus of this paper is such a system, as discussed in the next section.

A preview-based approach for non-minimum phase continuous-time systems was developed in a series of papers [6], [7], [8]. These papers derive a method of obtaining an unstable command-shaping filter, which is then decomposed into stable and unstable parts by partial fraction decomposition. To quote from [7], "The bounded solution to the optimal inversion problem is then obtained by flowing the stable portion forward in time and flowing the unstable portion backward in time." In the third paper, [8], a method is given for computing an "optimal boundary condition," which is used to greatly reduce the preview time of the method given in [6], [7]. The optimal boundary condition is a matrix integral expression involving the reference input and several of its derivatives. These papers do not say anything about the digital implementation of the approach, e.g., the sampling rate necessary to perform the required integral calculations with sufficient accuracy.

The discrete-time approach presented in the previous subsection performs nearly perfect inversion over a certain bandwidth using a single command shaping filter driven by samples of the reference trajectory. A Bode plot of the cascade of the CSF and closed-loop system shows the bandwidth over which nearly perfect tracking can be obtained. The CSF can be used with any reference signal whose frequency content is contained within this bandwidth. A disadvantage of the proposed approach is that the bandwidth cannot be arbitrarily specified. It is determined by the value of d needed to obtain a stable CSF (see (20)). However, for the H-frame system presented in the next section, as well as for the example systems used in [6], [7], [8], the method presented in this paper provides a bandwidth that is adequate to track the desired reference signals.

IV. Experimental Results

In this section we carry out the design and implementation of a tracking control system for an H-Frame XY positioning system. This system consists of two stationary motors, eight pulleys, and a single drive belt, as shown in Fig. 3. A

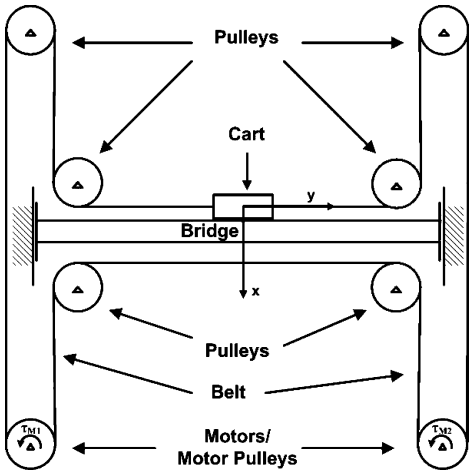

Fig. 3. An H-frame XY positioning system.

detailed description of the derivation of an 8th-order state-space model is given in [1]. That paper gives the $(\mathbf{A}, \mathbf{B}, \mathbf{C})$ plant model, and also describes some nonlinear friction in the hardware system. The design methodology in this paper does not explicitly incorporate the nonlinear friction. It is, of course, present in the hardware results shown in the

following subsection. The feedback loop is designed with sufficient bandwidth to ameliorate the effects of friction while not exciting unmodeled high-frequency dynamics due to the compliance of the drive belt. A picture of the hardware system is given in Fig. 4.

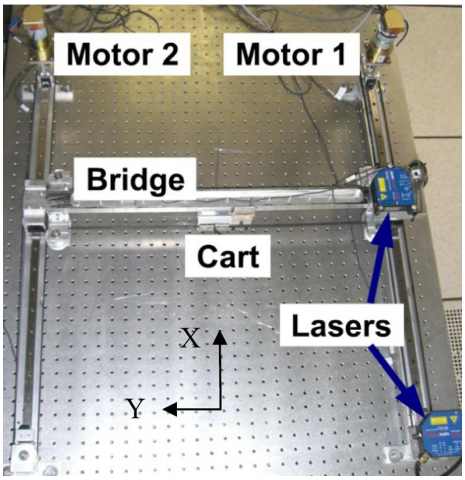

Fig. 4. The experimental H-frame XY positioning system.

The inputs, outputs, and state variables for this plant are:

$$\begin{aligned} x_1 &= x \text{ postition of cart (m)} \\ x_2 &= x \text{ velocity of cart (m/s)} \\ x_3 &= y \text{ postition of cart (m)} \\ x_4 &= y \text{ velocity of cart (m/s)} \\ x_5 &= \text{angular position of motor 1} \\ x_6 &= \text{angular velocity of motor 1} \\ x_7 &= \text{angular position of motor 2} \\ x_8 &= \text{angular velocity of motor 2} \end{aligned}$$

The inputs are the voltages to the two motor power amplifiers, and the tracked outputs are the x and y positions of the cart, which are measured by laser position sensors whose voltage outputs are sampled by 12-bit A/D converters. The motor positions are measured with optical encoders. Velocity signals are obtained from the corresponding position signals using a reduced-order observer. The sampling interval was chosen to be $T = 5 \times 10^{-4}$ seconds.

The design model shown in (6) includes the additional dynamics, which are two integrators, giving a 10th-order design model. The feedback gain matrix $\mathbf{K}_d$ is calculated using discrete-time linear quadratic regulator theory with the following weight matrices:

$$\mathbf{Q} = 1000 \cdot \text{ diag}(0,0,0,0,0,0,0,0,1,1), \ \mathbf{R} = \text{ diag}(1,1). \quad (21)$$

With the gain matrices $\mathbf{K}_1$ and $\mathbf{K}_2$ obtained by partitioning $\mathbf{K}_d$ (see (7)), the closed-loop system (8) is formed. Its zeros (rounded to two decimal digits) are:

$$-9.80, -0.99, -0.99, -0.10, -0.10.$$

This closed-loop system can be inverted exactly with a delay of $r = 2$ samples. However, the zero located at -9.8 will be an unstable pole of the exact inverse model. Furthermore, an exact inverse would have poles at the locations of the zeros of the modified plant on the negative real axis, resulting in a highly oscillatory output signal from the inverse model.

Using the procedure described in Section III, it is found that 18 additional delays, $s = 18$, are needed to make the CSF have poles whose magnitude is less than or equal to 0.99. With $d = r + s = 20$ delays, the preview time is $20T = 0.01$ sec. The Bode plot of the cascade of the CSF and the closed-loop system is shown in Fig. 5. Zooming in on

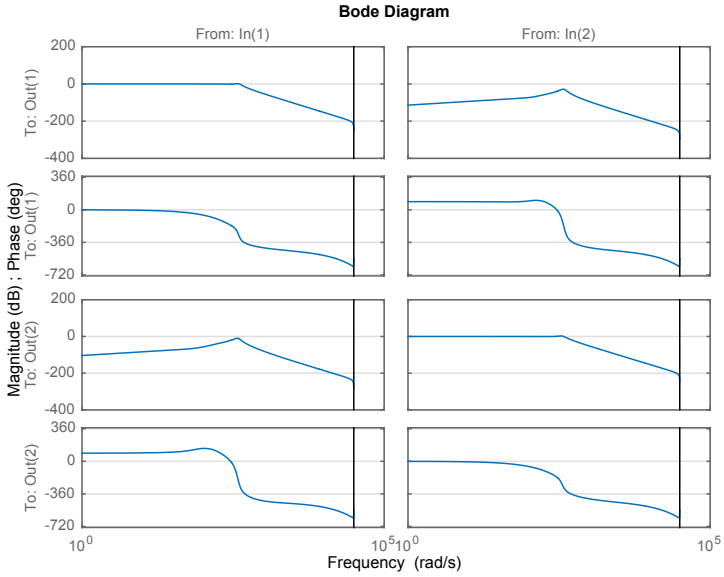

Fig. 5. Bode plots of the 2-input, 2-output system consisting of the cascade of the CSF and closed-loop system. See Fig. 2.

the plot shows that precision tracking can be achieved over a bandwidth of 0 to 60 rad/sec or about 10 Hz. It should be noted that the feedback system without the CSF has a precision tracking bandwidth of about 2 Hz. Thus, the CSF has extended the bandwidth by a factor of 5.

Fig. 6 shows the reference trajectories that cause the cart to move along a square whose sides have length 2.5 cm. An FFT of these reference trajectories shows that more than 98% of their energy is contained in the frequency range from 0 to 6 Hz, which fits within the 10 Hz precision tracking bandwidth provided by the cascade of the CSF and feedback loop designed above.

The reference signals were used with the hardware H-frame system and the resulting x and y displacements are shown in Fig. 7.

The motor angles recorded throughout the trajectory are shown in Fig. 9. Note that the regions of constant x and y shown in Fig. 7 are produced by the motor signals in Fig. 9, which are never constant. The two motors must move in a coordinated fashion to obtain regions of constant x or y. The input signals to the two motors are shown in Fig. 10, and the resulting xy position of the end effector is shown in Fig. 11.

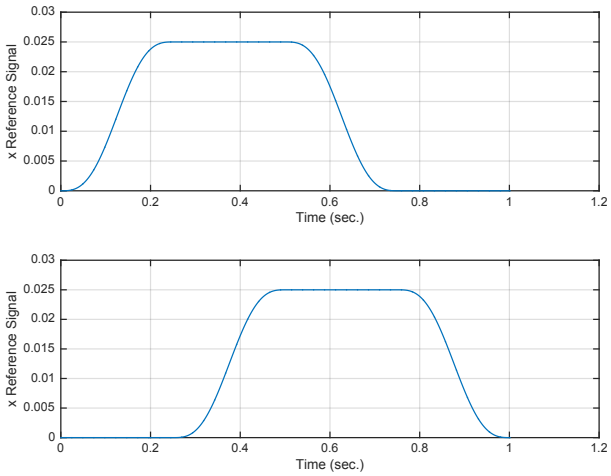

Fig. 6. The x and y reference trajectories for end-effector motion consisting of a 2.5 cm square.

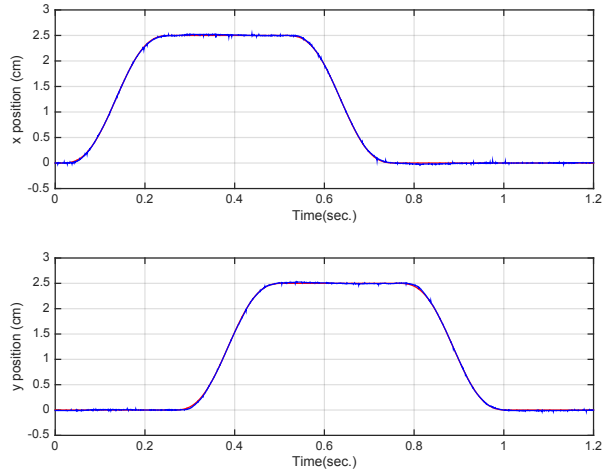

Fig. 7. Experimental x and y reference (red) and achieved (blue) trajectories for the H-frame system. Note that the blue curve is plotted over the red curve and that the spikes in the blue plot are attributed to sensor noise. The tracking errors are shown in Fig. 8.

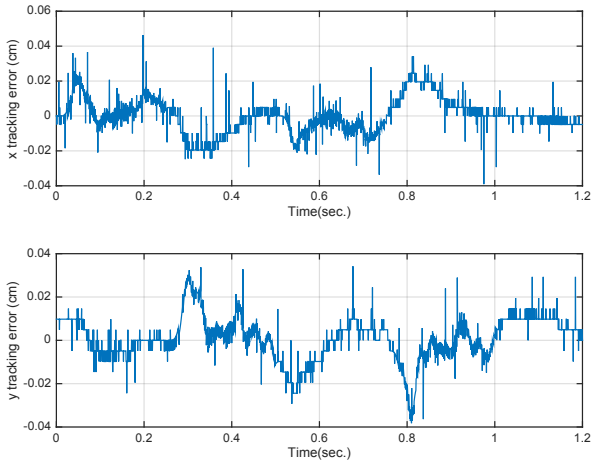

Fig. 8. Experimental x and y tracking errors for the H-frame system in response to the reference signals given in Fig. 6.

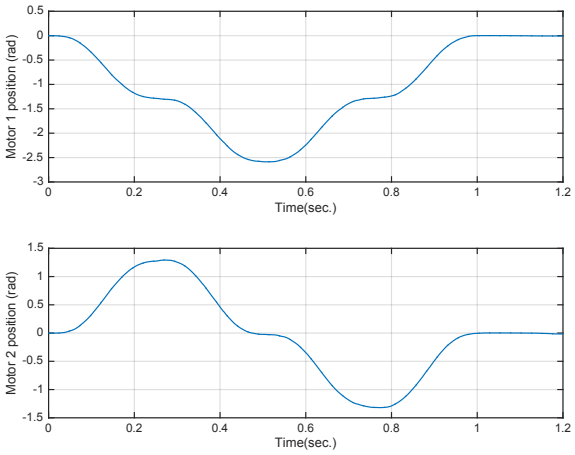

Fig. 9. Experimental motor position signals for the H-frame system in response to the reference signals given in Fig. 6.

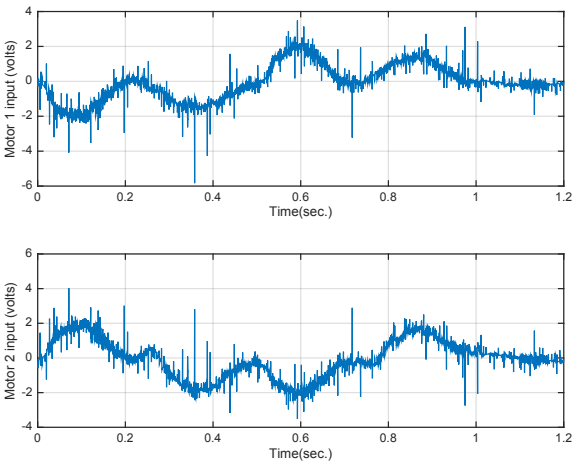

Fig. 10. Experimental motor input signals for the H-frame system in response to the reference signals given in Fig. 6.

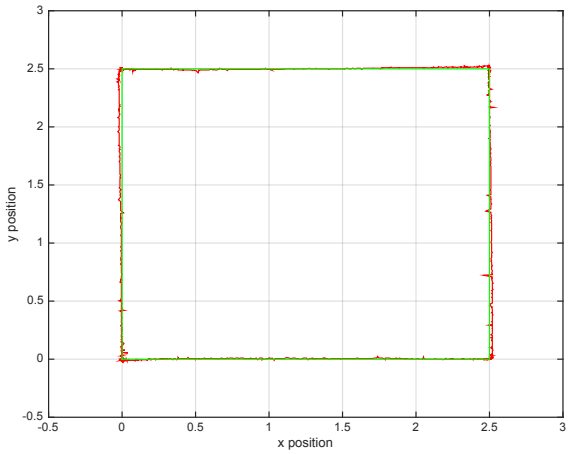

Fig. 11. xy position of the end effector (red) and desired xy position (green) corresponding to the reference signals shown in Fig. 6. The spikes in the end-effector plot are attributed to sensor noise.

V. Conclusions

We have presented the design and implementation of precision-tracking control for an H-frame XY positioning system. The control system architecture is the cascade of a command-shaping filter and a feedback tracking system. The feedback system was designed using standard linear quadratic methods with integral control. The precision-tracking bandwidth of the feedback system alone was about 2 Hz. A procedure was given for designing a command shaping filter. Cascading this filter with the feedback system extended the precision-tracking bandwidth of the H-frame system to 10 Hz.

References

[1] K.S. Sollmann, M.K. Jouaneh, and D. Lavender, "Dynamic Modeling of a Two-Axis, Parallel, H-Frame-Type XY Positioning System," *IEEE/ASME Trans. Mechatronics*, vol. 15, no. 2, pp. 280–290, April, 2010.

[2] E.J. Davison and A. Goldenberg, "Robust Control of a General Servomechanism Problem: the Servo Compensator," *Automatica*, vol. 11, pp. 461—471, 1975.

[3] R.J. Vaccaro, *Digital Control: A State-Space Approach*, McGraw-Hill, New York, NY; 1995.

[4] E. Zattoni, "Geometric Methods for Invariant-Zero Cancellation in Linear Multivariable Systems with Application to Signal Rejection with Preview," *Asian Journal of Control*, vol. 16, no. 5, pp. 1289-129, September 2014.

[5] G. Marro, D. Prattichizzo, and E. Zattoni, "Convolution Profiles for Right Inversion of Multivariable Non-Minimum Phase Discrete-Time Systems," *Automatica*, vol. 38, pp. 1695-1703, 2002.

[6] Q. Zou and S. Devasia, "Preview-Based Stable-Inversion for Output Tracking," in *Proc. American Control Conf.*, pp. 3544-3548, June 1999.

[7] Q. Zou and S. Devasia, "Preview-Based Optimal Inversion for Output Tracking: Application to Scanning Tunneling Microscopy," *IEEE Trans. Control Systems Technology,* vol. 12, no. 3, pp. 375-386, May 2004.

[8] Q. Zou, "Optimal Preview-Based Stable-Inversion for Output Tracking of Nonminimum-Phase Linear Systems," *Automatica*, vol. 45, pp. 230-237, 2009.